AMERICAN SOCIETY FOR MICROBIOLOGY | Antimicrobial Agents and Chemotherapy®

EXPERIMENTAL THERAPEUTICS

Impact of Type III Secretion Effectors and of Phenoxyacetamide Inhibitors of Type III Secretion on Abscess Formation in a Mouse Model of *Pseudomonas aeruginosa* Infection

Bryan J. Berube,[a]* Katherine R. Murphy,[a] Matthew C. Torhan,[c] Nicholas O. Bowlin,[c] John D. Williams,[c] Terry L. Bowlin,[c] Donald T. Moir,[c] Alan R. Hauser[a,b]

Departments of Microbiology/Immunology[a] and Medicine,[b] Northwestern University, Chicago, Illinois, USA; Microbiotix, Inc., Worcester, Massachusetts, USA[c]

ABSTRACT *Pseudomonas aeruginosa* is a leading cause of intra-abdominal infections, wound infections, and community-acquired folliculitis, each of which may involve macro- or microabscess formation. The rising incidence of multidrug resistance among *P. aeruginosa* isolates has increased both the economic burden and the morbidity and mortality associated with *P. aeruginosa* disease and necessitates a search for novel therapeutics. Previous work from our group detailed novel phenoxyacetamide inhibitors that block type III secretion and injection into host cells *in vitro*. In this study, we used a mouse model of *P. aeruginosa* abscess formation to test the *in vivo* efficacy of these compounds against the *P. aeruginosa* type III secretion system (T3SS). Bacteria used the T3SS to intoxicate infiltrating neutrophils to establish abscesses. Despite this antagonism, sufficient numbers of functioning neutrophils remained for proper containment of the abscesses, as neutrophil depletion resulted in an increased abscess size, the formation of dermonecrotic lesions on the skin, and the dissemination of *P. aeruginosa* to internal organs. Consistent with the specificity of the T3SS-neutrophil interaction, *P. aeruginosa* bacteria lacking a functional T3SS were fully capable of causing abscesses in a neutropenic host. Phenoxyacetamide inhibitors attenuated abscess formation and aided in the immune clearance of the bacteria. Finally, a *P. aeruginosa* strain resistant to the phenoxyacetamide compound was fully capable of causing abscess formation even in the presence of the T3SS inhibitors. Together, our results further define the role of type III secretion in murine abscess formation and demonstrate the *in vivo* efficacy of phenoxyacetamide inhibitors in *P. aeruginosa* infection.

KEYWORDS *Pseudomonas aeruginosa*, abscesses, neutrophils, phenoxyacetamide inhibitors, type III secretion

Received 9 June 2017 **Returned for modification** 30 June 2017 **Accepted** 4 August 2017

Accepted manuscript posted online 14 August 2017

Citation Berube BJ, Murphy KR, Torhan MC, Bowlin NO, Williams JD, Bowlin TL, Moir DT, Hauser AR. 2017. Impact of type III secretion effectors and of phenoxyacetamide inhibitors of type III secretion on abscess formation in a mouse model of *Pseudomonas aeruginosa* infection. Antimicrob Agents Chemother 61:e01202-17. https://doi.org/10.1128/AAC.01202-17.

Address correspondence to Alan R. Hauser, ahauser@northwestern.edu.

* Present address: Bryan J. Berube, Infectious Disease Research Institute, Seattle, Washington, USA.

Pseudomonas aeruginosa is one of the leading causes of nosocomial infections, responsible for over 50,000 cases and 400 deaths annually in the United States alone (1). Infections with *P. aeruginosa* can manifest in a number of ways, including hospital-acquired pneumonia, bacteremia, urinary tract infections, and ocular disease. *P. aeruginosa* can also cause a spectrum of infections that involve macro- or microabscess formation, including intra-abdominal infections, wound infections, hot tub folliculitis, and hot-foot syndrome (2–4). *P. aeruginosa* infections have become more dangerous and costly to treat due to the rise in antibiotic resistance; in a recent study, 13% of isolates were multidrug resistant (5). This alarming trend has led to the inclusion of *P. aeruginosa* as a member of the ESKAPE (*Enterococcus faecium*, *Staphylococcus aureus*,

Klebsiella pneumoniae, *Acinetobacter baumannii*, *Pseudomonas aeruginosa*, and *Enterobacter* species) pathogens, a group of six bacterial pathogens most in need of novel therapies (6). As a result, there is a pressing need to identify novel ways to treat *P. aeruginosa* disease.

One of the major virulence factors employed by *P. aeruginosa* to attack the host is the type III secretion system (T3SS), which has been shown to contribute to the pathogenesis of *P. aeruginosa*-mediated sepsis, pneumonia, and ocular disease (7). The *P. aeruginosa* T3SS comprises a set of nearly 40 genes, which encode and regulate a supramolecular needle structure that protrudes from the surface of the bacterium. The type III needle, comprised of repeated subunits of the protein PscF, interacts with the secreted translocation proteins PopB and PopD to presumably form a conduit through which the four well-characterized type III effector proteins can travel directly from the bacterial cytosol into the host cell (7). The type III effector proteins ExoS and ExoT are bifunctional proteins with GTPase-activating protein (GAP) and ADP-ribosyltransferase (ADPRT) activities, ExoU is a phospholipase, and ExoY is an adenylate cyclase. One of the pathogenic roles played by the *P. aeruginosa* T3SS is to intoxicate host innate immune cells, such as neutrophils and macrophages, to prevent phagocytosis, thereby allowing bacterial persistence and dissemination from the site of infection (8–11).

The increasing rates of antimicrobial resistance among *P. aeruginosa* strains underscore the need to identify novel therapeutic agents effective against this pathogen. Phenoxyacetamide inhibitors are attractive candidates in this regard. These compounds are small molecules that potently inhibit *P. aeruginosa* type III secretion and the translocation of effector proteins into mammalian cells (12–14). These inhibitors not only have good activity against *P. aeruginosa* type III secretion and translocation (the 50% inhibitory concentrations [IC_{50}s] of some compounds are in the nanomolar range) but also have very good selectivity, with some compounds showing no toxicity to eukaryotic cells at concentrations up to 100 μM (14). Characterization of mutant strains resistant to phenoxyacetamide inhibitors identified a group of amino acid substitutions (V62I, R75C, R75H, and G80D) in PscF, thus providing strong evidence that the needle protein is the target of phenoxyacetamide inhibitors (13).

Recently, a mouse model of *P. aeruginosa* abscess formation in which neutrophils and the T3SS played a prominent role was described (15). In the study described here, we used this mouse model of abscess formation to study the *in vivo* efficacy of phenoxyacetamide inhibitors. These findings show the potential of these inhibitors for therapeutic use in *P. aeruginosa* infections.

RESULTS

***P. aeruginosa* establishes subcutaneous abscesses.** *P. aeruginosa* has the capacity to form abscesses in humans and mice (15). We therefore determined whether *P. aeruginosa* clinical isolate PA99 formed abscesses following subcutaneous injection into C57BL/6J mice. Subcutaneous injection of PA99 led to the formation of an abscess that protruded from the body of the mouse and reached its peak size within the first 24 h (Fig. 1A and B). Although the abscess decreased in size by day 2, overt signs of the abscess remained until 2 weeks postinfection (Fig. 1A). Histopathological analysis from day 1 showed an infiltration of host immune cells just under the skin at the site of infection (Fig. 1C). The abscesses did not progress to cause dermonecrotic lesions, as the surface of the skin remained intact (Fig. 1B and C). The abscess and immune infiltrate appeared to increase by day 3 by histopathological examination (Fig. 1C), despite a decrease in the total abscess area (Fig. 1A). By day 14 the abscess had resolved (Fig. 1A and C). We next enumerated bacterial loads by performing punch biopsies of the abscesses and surrounding tissues, homogenizing these samples, and plating them on agar for bacterial enumeration. One day following infection with 1.2×10^6 CFU, we recovered slightly less than 1×10^5 bacteria from the abscesses (approximately 10% of the initial inoculum) (Fig. 1D). The initial decrease in the bacterial load could be due to the dispersal of bacteria away from the site of infection or to innate immune cell clearance of a portion of the inoculum. Despite the reductions in the overall abscess

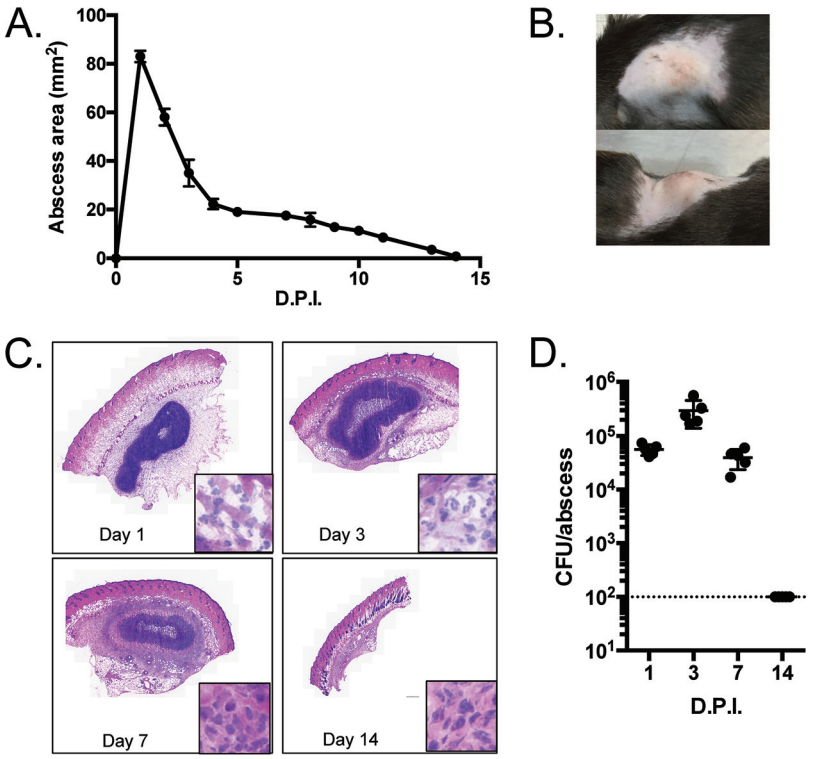

FIG 1 Characteristics of subcutaneous abscesses caused by *P. aeruginosa* strain PA99 in mice. (A to D) C57BL/6J mice were injected in the subcutaneous space with 1.2×10^6 CFU of *P. aeruginosa* strain PA99. (A) The abscess size was determined daily by measuring the length and width of the abscess. Five mice were used per group. Symbols represent means, and error bars represent standard errors of the means. (B) Photographs of representative abscesses. (C) Abscess tissues were harvested at the indicated times postinfection via punch biopsy and were subjected to H&E staining. For each panel, the inset shows a portion of the micrograph at enhanced magnification. (D) Abscess tissues were harvested at the indicated times postinfection, homogenized, and spot plated to assess the number of CFU. Each symbol represents a single mouse; five mice were used per group. The dotted line represents the limit of detection. For all experiments, the data shown are representative of those from at least three independent experiments. D.P.I., days postinfection.

sizes on days 2 and 3, the bacterial loads in these abscesses actually increased by 0.5 to 1 log CFU (Fig. 1D). These findings indicate that the large initial increase in abscess size was likely due to inflammatory infiltration that began to resolve by day 2. By day 7, the host began to clear the bacteria, resulting in recovered numbers of CFU similar to those observed on day 1 (Fig. 1D), and within 2 weeks the numbers of CFU in the abscesses were below the limit of detection (Fig. 1D). This correlated with the disappearance of any noticeable abscess on the surface of the skin by 14 days (Fig. 1A and C). Taken together, these data show that *P. aeruginosa* strain PA99 is capable of causing subcutaneous abscesses that are contained by the host immune response and that resolve by 2 weeks.

Neutrophils are recruited to the nascent abscesses. Given the apparent influx of inflammatory cells during PA99 abscess formation, we next examined whether neutrophils were recruited to the abscesses caused by PA99. To do this, we homogenized skin abscesses following infection and quantified the levels of a cytokine responsible for neutrophil recruitment (interleukin-1β [IL-1β]) and the levels of activity of a neutrophil effector (myeloperoxidase [MPO]). We found significantly elevated levels of both IL-1β (Fig. 2A) and MPO (Fig. 2B). The levels of IL-1β waned after the first day and returned to background levels by day 14 (Fig. 2A), again consistent with inflammation being a major driver of abscess size early in infection.

Type III secretion is required for abscess formation. We next examined whether the T3SS was required for abscess formation by PA99. The T3SS is an attractive

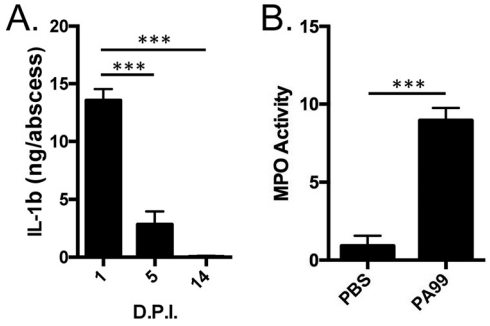

FIG 2 Inflammatory responses in nascent abscesses. C57BL/6J mice were infected in the subcutaneous space with strain PA99. (A) Abscess tissues were harvested and homogenized at the indicated times postinfection, and IL-1β levels were determined by ELISA. Data are means plus standard errors of the means. Experiments were done on three mice per group and were performed at least twice. Statistical analyses were performed by a one-way ANOVA and Dunnett's multiple-comparison test. ***, $P < 0.001$ compared to day 1. (B) Abscess tissues were harvested and homogenized at 24 h postinfection, and myeloperoxidase activity was measured as a surrogate for neutrophil activity. Experiments were done on five mice per group. Data are means plus standard deviations. Data were analyzed by an unpaired *t* test. ***, $P < 0.001$. D.P.I., days postinfection; PBS, phosphate-buffered saline; MPO, myeloperoxidase.

candidate for such a role for two reasons: (i) it has previously been shown to contribute to multiple routes of *P. aeruginosa* infection, including abscess formation (15), and (ii) the *P. aeruginosa* T3SS is known to specifically target neutrophils during infection and block their ability to clear bacteria (10). Given the recruitment of neutrophils to the nascent abscess (Fig. 2B), it seemed likely that the T3SS would play a predominant role. An isogenic *P. aeruginosa* strain lacking all known type III effectors (strain PA99null) was compared to the parental PA99 strain in the abscess model. This mutant failed to cause significant abscess formation following infection (Fig. 3A), to establish a large inflammatory focus under the skin (Fig. 3B), and to persist in high numbers beyond 24 h (Fig. 3C). Additionally, PA99null did not elicit an increase in IL-1β production at the site of infection (Fig. 3D), which could explain the lack of inflammation and the corresponding overt signs of abscess formation.

The T3SS of *P. aeruginosa* PA99 secretes three known effector proteins: ExoS, ExoT, and ExoU. We made use of a series of deletion mutants to elucidate which type III effectors contribute most to abscess formation. A PA99Δ*exoT* strain that secretes ExoS and ExoU (strain PA99SU) caused abscess formation indistinguishable from that caused by wild-type PA99 (Fig. 4A); the sizes of the abscesses caused by these two strains on day 1 postinfection were nearly identical (Fig. 4B). This indicates that ExoT is dispensable for abscess formation. However, ExoS and ExoU are necessary for full virulence, as both the PA99Δ*exoS* strain (strain PA99TU) and the PA99Δ*exoU* strain (strain PA99ST) caused significantly smaller abscesses throughout the 2-week follow-up period (Fig. 4A), with PA99Δ*exoU* causing the smallest abscesses of all strains (Fig. 4B). To test for the sufficiency of the type III effectors for abscess formation, we used PA99null strains engineered to secrete a single type III effector protein. As seen in Fig. 4, a strain secreting only ExoT was unable to cause abscess formation (Fig. 4C). The secretion of only ExoS resulted in the formation of abscesses of intermediate size, and the secretion of ExoU caused large abscesses indistinguishable from those observed at 1 day following infection with the parental PA99 strain (Fig. 4D). Together these data demonstrate that both ExoS and ExoU contribute to abscess formation, with ExoU being particularly important in this process.

Neutrophils prevent dissemination of PA99 bacteria during abscess formation. Neutrophils have been shown to play an important role in containing *P. aeruginosa* during infections, including during abscess formation (15), and the data in Fig. 1 and 2 suggest that neutrophils are recruited to abscesses caused by strain PA99. These immune cells are typically recruited to sites of bacterial infection, where they act to rapidly kill bacteria. However, the *P. aeruginosa* T3SS injects effector proteins into

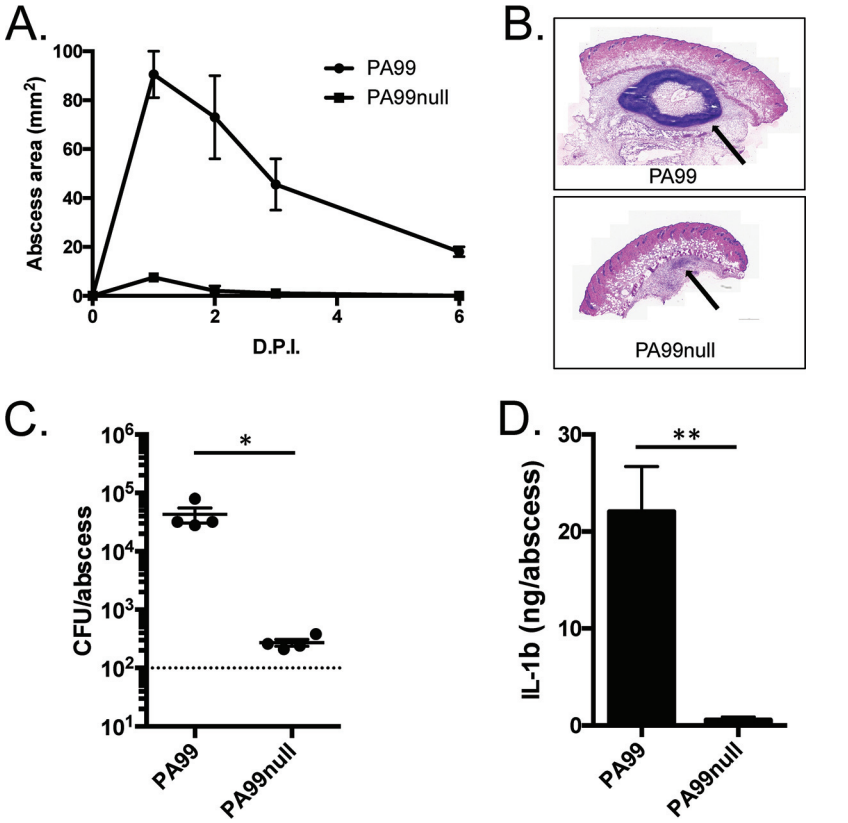

FIG 3 The role of type III secretion in abscess formation. C57BL/6J mice were infected in the subcutaneous space with either PA99 or PA99null. (A) The abscess size was measured daily over a 2-week period. Data are the mean abscess sizes for 5 mice per group, and error bars represent standard errors of the means. (B) Abscess tissues were harvested at 24 h postinfection, and cross sections of the abscesses were stained with H&E. Arrows, the abscess formed under the skin. (C) Abscess tissues were harvested by punch biopsy, and bacterial loads were determined by plating serial dilutions of tissue homogenates. Each symbol represents the abscess from a single mouse. Data are means plus standard deviations and were analyzed using an unpaired *t* test. Experiments used four mice per group and were performed at least three times. *, $P < 0.05$. (D) Abscess tissues were harvested at 24 h postinfection and homogenized. IL-1β levels were determined by ELISA. Data are means plus standard errors of the means and were analyzed using unpaired *t* tests. *, $P < 0.05$; **, $P < 0.01$. Experiments were done on three mice per group and were performed at least twice. D.P.I., days postinfection.

neutrophils, leading to inhibition of the uptake and killing of bacteria by phagocytosis, as well as to neutrophil death (11, 16–18). To investigate the importance of neutrophils in abscesses caused by strain PA99, we injected mice with an antibody against the neutrophil surface marker Ly6G, which serves to deplete the host of circulating neutrophils. Following neutrophil depletion, infection with PA99 led to abscesses twice as large as those observed in mice treated with an IgG control antibody (Fig. 5A). Additionally, by 2 days postinfection, mice with depleted circulating neutrophils developed dermonecrotic lesions on the skin overlying the abscesses (Fig. 5B, inset), which was not seen in control mice (Fig. 5B). The bacterial loads in the abscesses of neutrophil-depleted mice were $>1 \times 10^6$ CFU, a significant increase of 1.5 $\log_{10}$ CFU compared to the loads in the controls (Fig. 5C). Most importantly, neutrophil depletion allowed bacterial dissemination away from the site of infection and into the bloodstream, as bacteria were isolated from the liver and occasionally from the spleen following neutrophil depletion (Fig. 5D and E). These data show that neutrophils are required to curb bacterial proliferation at the site of infection, to limit damage to the surrounding skin tissue, and to prevent bacterial dissemination.

The T3SS is not required for disease in a neutropenic host. The data presented above show a complex interaction between host neutrophils and the bacterial T3SS

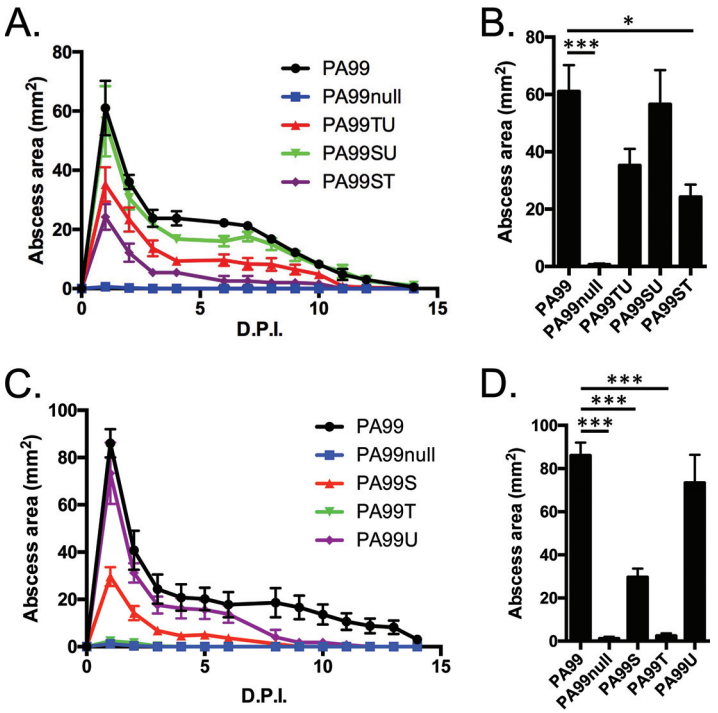

FIG 4 Roles of type III secretion effector proteins in abscess formation. C57BL/6J mice were infected in the subcutaneous space with *P. aeruginosa* strains lacking either a single type III effector (A and B) or two type III effectors (C and D). (A, C) Abscess sizes were measured over a 2-week period, and the peak abscess sizes at 24 h postinfection (from panels A and C) were plotted in bar graphs (B and D). The data in panels A and C represent mean abscess areas at each time point, and error bars represent standard errors of the means. The data in panels B and D represent means plus standard errors of the means and were analyzed by one-way ANOVA and Dunnett's multiple-comparison test. *, $P < 0.05$; ***, $P < 0.001$. Experiments were done on five mice per group. D.P.I., days postinfection.

during abscess formation. Neutrophil infiltration into tissue is clearly required to contain the infection. However, the predominant virulence factors contributing to abscess formation are the T3SS and the type III effectors ExoS and ExoU, which are known to specifically target and incapacitate neutrophils. We hypothesized that in the context of a neutropenic host, the T3SS might become dispensable and no longer essential for *P. aeruginosa* abscess formation. To test this possibility, we infected neutropenic mice with PA99null, which does not secrete T3SS effector proteins. Indeed, infection of neutropenic mice with PA99null not only caused abscesses that were similar in size to those found in neutropenic mice infected with wild-type PA99 (Fig. 6A) but also caused dermonecrotic lesions on the surface of the skin (Fig. 6B). Bacterial enumeration showed that PA99null bacteria proliferated to levels equivalent to those of wild-type PA99 bacteria in a neutropenic host (Fig. 6C); the bacterial loads recovered from both of these groups were significantly higher than those recovered from PA99-infected control mice. These data suggest that T3SS effector proteins counteract the role of neutrophils during abscess formation.

A type III secretion inhibitor protects against abscess formation. The preceding results demonstrate that the T3SS prevents neutrophils from efficiently clearing *P. aeruginosa* strain PA99 during abscess formation. The mouse model of abscess formation is therefore an ideal system to test the efficacy of compounds that inhibit the T3SS. We used several phenoxyacetamide inhibitors of type III secretion for this purpose. The inhibitor MBX 2359 has been previously described (12), while MBX 3459 and MBX 3357 are derivatives synthesized for the current study (Fig. 7; see Materials and Methods). MBX 3358, a stereoisomer of MBX 3357 that lacks type III secretion inhibitory activity, was synthesized as a negative control (Fig. 7). Four *P. aeruginosa* strains were used in these assays because of the availability of mutants with specific *pscF* alleles: MDM2423,

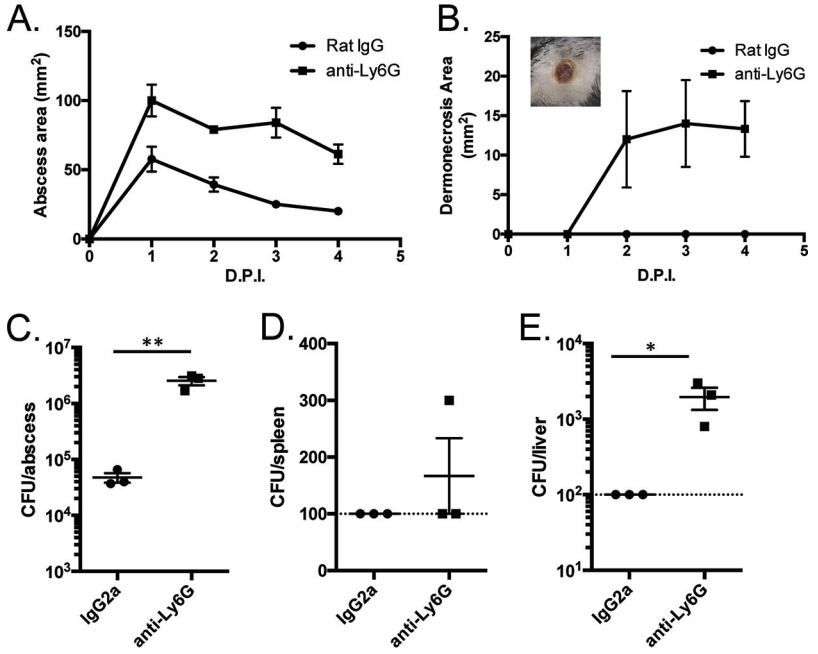

FIG 5 Characteristics of abscesses in neutropenic mice. C57BL/6J mice were injected in the peritoneum with IgG2a control antibodies or anti-Ly6G antibodies to deplete the neutrophils. The mice were then infected in the subcutaneous space with *P. aeruginosa* strain PA99. (A, B) Abscess areas (A) and dermonecrotic areas (B) were measured daily following infection. (B, inset) Picture of a representative dermonecrotic skin lesion from an anti-Ly6G antibody-treated mouse. (C to E) Abscess (C), spleen (D), and liver (E) tissues were homogenized at 24 h postinfection and plated for CFU enumeration. The dashed lines represent the limit of detection. Data are means plus standard errors of the means. Experiments were done on three mice per group and were performed at least twice. Data were analyzed by unpaired *t* tests. *, $P < 0.05$; **, $P < 0.01$. D.P.I., days postinfection.

a PA99null strain engineered to secrete ExoS tagged with a β-lactamase domain; MDM2424, a strain that is similar to MDM2423 but that lacks type III secretion activity because of a deletion of the *pscF* gene; MDM2438, a strain similar to MDM2423 but with a *pscF* allele encoding a PscF variant containing a single amino acid substitution (I63T) that confers resistance to the phenoxyacetamide inhibitors; and MDM2591, a strain isogenic to MDM2438 but with a wild-type *pscF* allele.

First, the ability of the inhibitors to block type III secretion *in vitro* was verified. MDM2423 was grown under conditions that induced type III secretion in the presence or absence of inhibitors. MBX 2359, MBX 3459, and MBX 3357 each reduced the amounts of secreted effector and translocation proteins observed in the supernatants of bacterial cultures, while MBX 3358, the inactive stereoisomer of MBX 3357, failed to do so (Fig. 8A). When injected into the site of infection along with *P. aeruginosa* strain PA99, the inhibitors MBX 2359, MBX 3459, and MBX 3357 all led to the formation of significantly smaller abscesses (Fig. 8B). For example, on day 1 postinfection, inhibitor-treated mice had abscesses that were approximately 50% smaller than those observed in untreated mice (Fig. 8C). The nonactive stereoisomer, MBX 3358, which failed to block type III secretion *in vitro*, also failed to inhibit abscess formation *in vivo*. These results indicate that phenoxyacetamide inhibitors have *in vivo* efficacy against *P. aeruginosa* in the context of abscess formation.

Previous work suggested that the phenoxyacetamide inhibitors specifically target the type III needle, as resistance mutations mapped to the *pscF* gene (which encodes the monomer that comprises the T3SS needle) (13). We utilized one of these phenoxyacetamide-resistant mutants [MDM2438*pscF*(I63T)] to confirm the *in vivo* specificity of the phenoxyacetamide inhibitors. The phenoxyacetamide-resistant mutant MDM2438 was refractory to inhibition by MBX 2359 in the model of abscess formation, with the sizes of the abscesses in MDM2438-infected mice being indistinguishable from

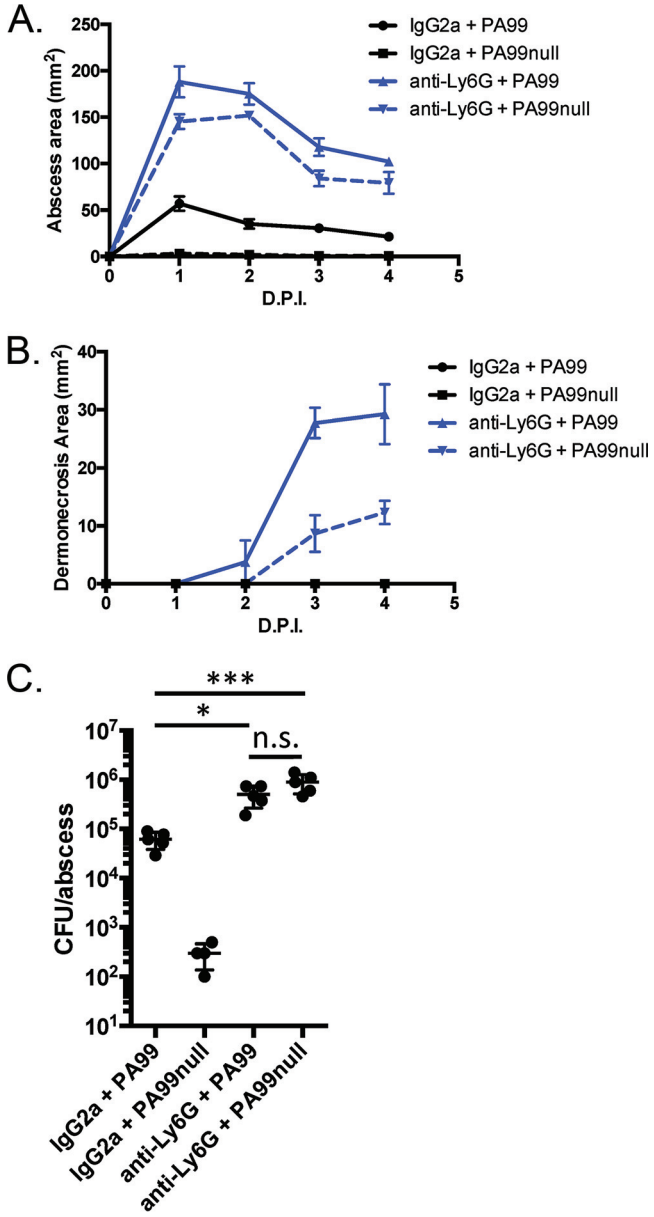

FIG 6 Role of type III secretion in abscess formation in a neutropenic mouse. C57BL/6J mice were injected in the peritoneum with IgG2a antibodies or anti-Ly6G antibodies to deplete the neutrophils. The mice were then infected in the subcutaneous space with *P. aeruginosa* strains PA99 or PA99null. (A, B) Abscess areas (A) and dermonecrotic areas (B) were measured daily following infection. (C) Mice were sacrificed at 24 h postinfection. Abscess tissues were harvested, homogenized, and plated for CFU enumeration. Data are means plus standard errors of the means. Statistics were calculated by a one-way ANOVA and Tukey's multiple-comparison test. *, $P < 0.05$, ***, $P < 0.001$; n.s., no significant difference. Four mice were used in the group treated with IgG2a and infected with PA99null; 5 mice per group were used for all other conditions. D.P.I., days postinfection.

those of the abscesses in control mice (Fig. 8D). In contrast, abscesses caused by MDM2591, which is identical to MDM2438 except that *pscF*(I63T) is replaced with a wild-type allele of *pscF*, were reduced in size by 50% (Fig. 8D). These findings indicate that phenoxyacetamide inhibitors attenuate *P. aeruginosa* abscesses by blocking type III secretion.

DISCUSSION

Once a bacterial pathogen has passed the skin barrier, the innate immune system is the next line of defense in the host's attempt to combat and control infection. Animal

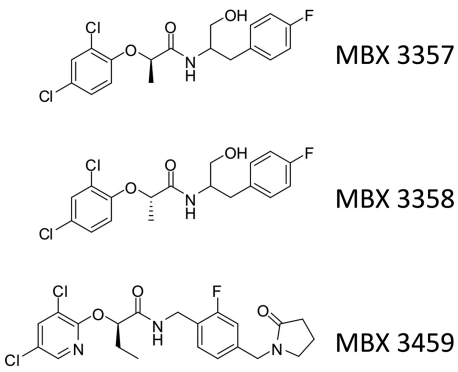

FIG 7 Structures of novel phenoxyacetamide inhibitors. The chemical structures of MBX 3357, MBX 3358, and MBX 3459 are shown. MBX 3357 and MBX 3459 have inhibitory activity; MBX 3358 is an inactive stereoisomer of MBX 3357.

models of *P. aeruginosa* infection in other organ systems have shown neutrophils to be the primary cell type responsible for the initial response to *P. aeruginosa* (7, 10, 11, 19). Our study shows this to be true in the skin and soft tissue as well and highlights an exquisite balance between the T3SS and host neutrophils during *P. aeruginosa* abscess formation. A functional T3SS is required for abscess formation and for the ability of *P.*

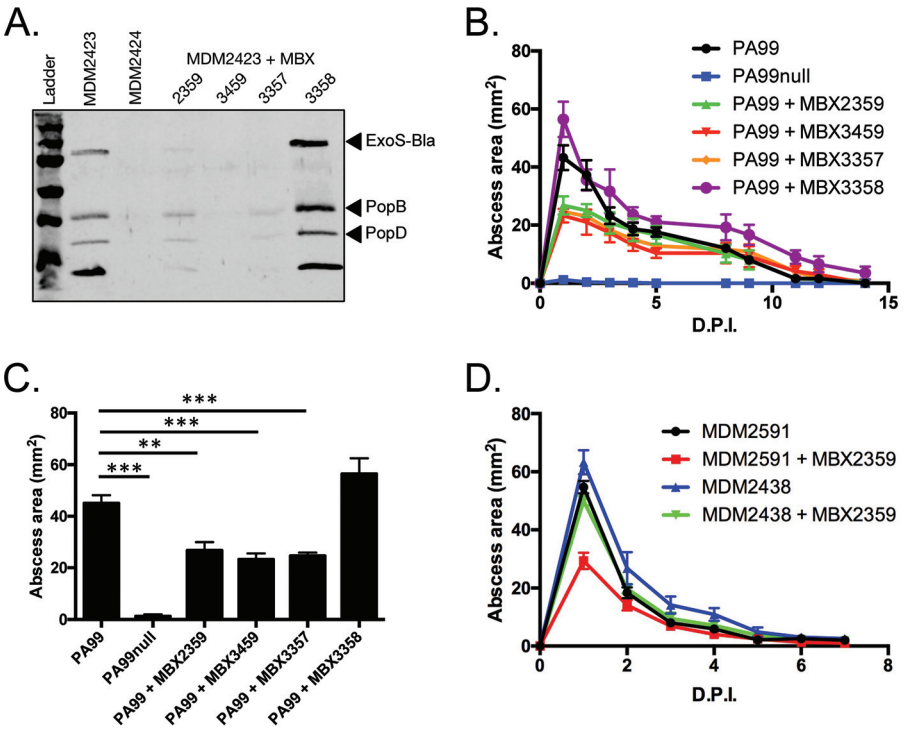

FIG 8 *P. aeruginosa* abscess formation in the presence of T3SS inhibitors. (A) *P. aeruginosa* strains were grown under secretion-inducing conditions in the presence or absence of T3SS inhibitors. The secretion of type III effectors into the supernatant was examined by Western blotting. (B, C) C57BL/6J mice were infected in the subcutaneous space with *P. aeruginosa* PA99 strains in the presence or absence of various phenoxyacetamide T3SS inhibitors (the final concentration of 100 μM was delivered in the inoculum), as indicated. Five mice were infected per group, and the experiment was repeated twice. (B) The abscess size was measured over the subsequent 2 weeks postinfection. (C) The peak abscess size (at day 1 postinfection) was plotted in a bar graph. (D) *P. aeruginosa* strains susceptible or resistant to phenoxyacetamide compounds were injected into the subcutaneous space of C57BL/6J mice in the presence or absence of the inhibitor MBX 2359. Experiments were performed on two different days, and the results were pooled. A total of 10 mice per group were used. The abscess size was measured over the subsequent 2 weeks. Data are means plus standard errors of the means. Statistics were calculated by a one-way ANOVA and Dunnett's multiple-comparison test. **, $P < 0.01$; ***, $P < 0.001$. D.P.I., days postinfection.

aeruginosa to persist within the subcutaneous tissues for up to 2 weeks, presumably by intoxicating neutrophils and preventing phagocytosis. However, neutrophil recruitment to the site of infection is ultimately host protective and serves to wall off the bacteria and prevent spread throughout the body. These results are consistent with those seen for other bacterial pathogens. During *Staphylococcus aureus* cutaneous infection, IL-1β secretion by keratinocytes and subsequent neutrophil recruitment help cause abscess formation but are ultimately host protective (20, 21); IL-1β depletion allows the bacterium to cause enlarged dermonecrotic lesions on the surface of the skin (20).

Our data support findings in a recent study by Pletzer and colleagues highlighting the importance of neutrophils in containing *P. aeruginosa* subcutaneous abscesses (15). They report that high doses of select *P. aeruginosa* clinical isolates are capable of causing dermonecrosis of the skin, as well as disseminated disease and lethality, in a subcutaneous infection model. In our subcutaneous abscess model, *P. aeruginosa* is unable to cause disseminated disease unless the mice are neutropenic. The difference could be due to the specific type III effectors present in the different strains or could be due to additional virulence factors that may augment type III-mediated disease. We show in the case of *P. aeruginosa* strain PA99 that the type III effector ExoU is sufficient to mediate abscess formation and that ExoS and ExoT are not required. Future studies should be aimed at determining the mechanism of ExoU-mediated disease and the temporospatial dynamics of *P. aeruginosa* host cell intoxication. During lung infection, *P. aeruginosa* intoxicates neutrophils early during infection to combat the initial innate immune response but subsequently intoxicates epithelial cells, which serves to breach the pulmonary-vascular barrier and allow dissemination to internal organs (10, 22). It would be interesting to determine whether other cell types become injected with effector proteins during *P. aeruginosa* skin and soft tissue infections and whether this contributes to neutrophil recruitment or bacterial dissemination, given what is known regarding *P. aeruginosa* lung and *S. aureus* subcutaneous infections.

P. aeruginosa causes a variety of infections that are associated with abscess formation, which supports the clinical relevance of the subcutaneous abscess model. Pseudomonas hot-foot syndrome occurs after a person wades in pools contaminated with *P. aeruginosa* and presents as a sudden onset of painful subcutaneous nodules on the soles of the feet (2). These nodules may involve microabscess formation (2). In these cases, patients generally clear the infection within 7 to 10 days, on par with what we saw in our model. While hot-foot syndrome is generally self-clearing, this type of infection is a potentially important public health hazard. Several studies have looked at the prevalence of *P. aeruginosa* isolates in public swimming pools, with some studies finding contamination in up to 60% of pools tested (23, 24). *P. aeruginosa* also causes intra-abdominal infections, wound infections, and hot tub folliculitis (2–4). These infections manifest with abscesses formed by dense infiltrations of neutrophils (3). In the case of hot tub folliculitis, abscesses can occasionally form even in the absence of a bacterial focus and generally leave the epidermis unharmed (3). The mouse model described above recapitulates the clinical findings of *P. aeruginosa* abscess formation and is thus a good model to study these disease processes.

In contexts in which innate defenses are compromised, such as in burn and wound patients or neutropenic hosts, severe and life-threatening complications of *P. aeruginosa* infections can arise (25). In our model, a neutropenic mouse is unable to contain bacterial replication and is incapable of preventing the spread of *P. aeruginosa* to the liver. Dissemination of bacteria in a neutropenic host is a common phenomenon in *P. aeruginosa* infections in animals and in human patients (26, 27). Ecthyma gangrenosum is a manifestation of *P. aeruginosa* bacteremia in which bacteria disseminate to and destroy tissues in the skin and soft tissues, resulting in open lesions (28). This disease is generally found in neutropenic patients; however, numerous cases have been seen in previously healthy individuals and even in those without overt bacteremia (28–32). We observed a similar phenomenon in neutropenic mice, in which *P. aeruginosa* was

not contained at the site of infection but spread to the skin and caused extensive damage leading to dermonecrotic lesions.

The rise in antibiotic resistance among Gram-negative bacteria has prompted the search for novel preventatives and therapeutics. The strategy of antagonizing T3SSs as a means to prevent or treat infection has garnered substantial interest in recent years because these systems often play important roles in pathogenesis and have several advantages as targets for inhibition. First, the T3SS needle resides on the surface of the bacterium, obviating the requirement for penetration through the bacterial outer membrane and avoidance of efflux pumps. Second, T3SSs are largely found in bacterial pathogens and not commensal bacteria, limiting the effects that inhibitors might have on the human microbiome. Third, given the conservation of T3SSs across bacterial species, individual inhibitors could potentially be active against multiple bacterial pathogens. It is therefore not surprising that a number of agents have been investigated for the purpose of inhibiting these systems (33). Of these, monoclonal antibodies are the most advanced in development. Antibodies against the needle tip protein, LcrV, protected mice against *Yersinia pestis* infection (34–36), while antibodies against the *P. aeruginosa* ortholog, PcrV, were effective in several animal models (37–39) and have been tested in clinical trials for the prevention of *P. aeruginosa* acute pneumonia in hospitalized patients and respiratory infections in individuals with cystic fibrosis (40, 41). A divalent antibody (MEDI3902) that recognizes both PcrV and the surface polysaccharide Psl is currently undergoing testing in a phase II clinical trial (42). Recent work has also focused on small-molecule inhibitors of type III secretion, as these types of therapeutics have the potential added advantage of oral bioavailability, whereas monoclonal antibodies need to be given by injection. Over the last 10 years, several small-molecule inhibitors of T3SSs have been developed and proven efficacious in reducing virulence in animal models of disease. Acylated hydrazones of salicylaldehyde (e.g., INP0007 and INP0403) prevent the secretion of type III effectors from *Salmonella enterica* serovar Typhimurium, thereby blocking invasion of epithelial cells and preventing infection (43); INP0341, a salicylidene acylhydrazide, inhibited the type III secretion of *Chlamydia trachomatis* and significantly reduced vaginal infections in mice. Aurodox, a linear polyketide compound, blocked the secretion of type III effectors and protected mice from a lethal dose of *Citrobacter rodentium* (44). Given the important role played by the T3SS in *P. aeruginosa* infections and the benefits of small-molecule drugs, it is anticipated that efforts will continue to focus on agents that inactivate this important virulence determinant. Our results demonstrate that the *P. aeruginosa* T3SS plays a pivotal role in abscess formation and that the mouse model of subcutaneous infection is useful for evaluating the *in vivo* efficacy of compounds that target this secretion system.

Phenoxyacetamide inhibitors are small molecules that potently and selectively inhibit type III secretion and injection *in vitro* by presumably targeting the needle protein PscF (12–14). Extensive structure-activity relationship studies have shown that the phenoxyacetamide scaffold is highly modifiable during hit-to-lead studies (12, 14). Select compounds exhibit IC_{50}s in the low-micromolar to high-nanomolar range with no cytotoxicity up to 100 μM (12, 14). We have now extended these studies to show that these small-molecule inhibitors have *in vivo* activity. It is noteworthy that the phenoxyacetamide inhibitors also block type III secretion in *Y. pestis* and prevent *C. trachomatis* intracellular growth, which is dependent on the T3SS (12). These data suggest that these inhibitors may be useful in the treatment of infections caused by several bacterial pathogens. In the future, it will be important to test these inhibitors in other models of disease and in conjunction with conventional antibiotics to broaden their usefulness in combating *P. aeruginosa* infection.

MATERIALS AND METHODS

Bacterial strains. *P. aeruginosa* strain PA99, a clinical isolate that naturally secretes ExoS, ExoT, and ExoU (45), was used for these studies. The type III secretion effector-encoding genes *exoS*, *exoT*, and *exoU* had been previously disrupted either individually or in combination to generate isogenic mutants that secrete ExoT and ExoU (strain PA99TU), ExoS and ExoU (strain PA99SU), ExoS and ExoT (strain PA99ST),

TABLE 1 Sequences of primers used in this study

Primer name	Sequence
exoU-Up-F+GWL	TACAAAAAAGCAGGCTGATTTTCTCCTGCCGGTACA
exoU-Up-R	TGTGAACTCCTTATTCCGCCGGATATGCATGTTCGCTCCT
exoU-Dwn-F	AGGAGCGAACATGCATATCCGGCGGAATAAGGAGTTCACA
exoU-Dwn-R+GWR	TACAAGAAAGCTGGGTAAACCCAGGAGGGTTCTGAG
exoU-Out-F	TGCTGTACGCCCAGACATAG
exoU-Out-R	ACGTCCTTCGACTGAAAACG

only ExoU (strain PA99U), only ExoS (strain PA99S), only ExoT (strain PA99T), or no effector proteins (strain PA99null) (45). All mutants had equivalent growth rates in Luria-Bertani (LB) medium and MINS medium (25 mM KH_2PO_4, 95 mM NH_4Cl, 50 mM monosodium glutamate, 110 mM disodium succinate, 10 mM trisodium nitrilotriacetic acid, 2.5% glycerol, 5 mM $MgSO_4$, 18 μM $FeSO_4$) (45). The construction of PA99 variants MDM2423, MDM2424, MDM2438, and MDM2591 is described below. For all animal experiments, bacteria were grown overnight at 37°C with shaking in MINS medium and then subcultured in fresh MINS medium for 2.5 h. For *in vitro* experiments, all bacteria were grown overnight in LB broth with shaking at 37°C.

Bacterial strain construction. MDM2423 (PA99null::mini-CTX-*exoS-bla*) was designed to allow quantification of secretion and translocation of the effector protein ExoS in the presence or absence of T3SS inhibitors. This PA99null variant contains an *exoS*–β-lactamase translational fusion allele inserted at a neutral site in the chromosome, which allows measurement of ExoS translocation into mammalian cells (10). MDM2423 was constructed as follows: a full-length copy of the *exoS* gene fused to the TEM1 β-lactamase (*bla*) gene was inserted into the vector mini-CTX1 (46) as described previously (13), except that a wild-type allele of *exoS* was used as the template for PCR amplification. The resulting mini-CTX-*exoS-bla* vector was integrated into the chromosomal *attB* site of PA99null (45) to yield strain MDM2423.

MDM2424 (PA99null Δ*pscF*::mini-CTX-*exoS-bla*), a PA99 variant with a deletion in the gene encoding the needle protein PscF and with the *exoS*–β-lactamase translational fusion allele inserted at a neutral site in the chromosome, was constructed as follows: an in-frame, markerless deletion of the *pscF* gene from strain PA99U (45) was generated by use of the standard Gateway and splicing by overlap extension PCR (SOE PCR) technology as described previously (13). The deletion was confirmed by sequencing to leave 2 amino-terminal and 7 carboxy-terminal codons of *pscF* fused in frame. Next, the *exoU* gene was deleted by means of the same SOE PCR method, except that the *exoU* primers listed in Table 1 were used. Sequencing confirmed that 3 amino-terminal and 7 carboxy-terminal codons were fused in frame in the deletion. Finally, the mini-CTX-*exoS-bla* construct was integrated into the chromosomal *attB* site to generate strain MDM2424.

MDM2438 [PA99null *pscF*(I63T)::mini-CTX-*exoS-bla*] contains a *pscF* allele that confers resistance to phenoxyacetamide inhibitors. It was constructed as follows: a *pscF* allele encoding PscF with an I63T substitution had been previously generated by error-prone PCR of the *pscF* gene with a GeneMorph II random mutagenesis kit (Agilent, Inc.) (13). This PscF variant had been shown to confer resistance to the phenoxyacetamide class of T3SS inhibitors (13) The allele conferring resistance, *pscF*(I63T), was moved from the random mutant library by PCR into vector pEXGWGm and used to replace the deleted *pscF* allele in MDM2424 via sucrose counterselection (47) to generate strain MDM2438.

MDM2591 (PA99null::mini-CTX-*exoS-bla*) is similar to MDM2423, except that it was generated in the same background as MDM2424 and MDM2438 to exclude the influence of off-site mutations on comparisons of these strains. MDM2591 was constructed similarly to MDM2424, except that the *pscF* gene was not deleted from PA99U. The same process of deleting the *exoU* gene and adding the mini-CTX-*exoS-bla* construct was applied to PA99U with an intact *pscF* gene.

Chemistry. Phenoxyacetamide MBX 2359 was described previously (13). Experimental details for synthesis of the novel compounds are presented in the following sections.

(i) Synthesis of MBX 3357 and MBX 3358. In separate reactions, (*R*)- and (*S*)-2-(2,4-dichlorophenoxy)propanoic acid (0.100 g, 0.425 mmol, 1.0 equivalents [eq]) were combined with commercially available 2-amino-3-(4-fluorophenyl)propan-1-ol (0.086 g, 1.2 eq), 1-[bis(dimethylamino)methylene]-1H-1,2,3-triazolo[4,5-b]pyridinium 3-oxid hexafluorophosphate (HATU; 0.194 g, 1.2 eq) and diisopropylethylamine (DIPEA; 0.1 ml, 1.3 eq) in dimethyl formamide (DMF; 2 ml) and maintained at room temperature. After approximately 18 h, the reaction mixtures were diluted with water and the resultant precipitates were collected and characterized. (i) *N*-[2-(4-Fluorophenyl)-1-(hydroxymethyl)ethyl]-2(*R*)-(2,4-dichlorophenoxy)propanamide (MBX 3357) 0.142 g (87%), off-white solid; ^{1}H nuclear magnetic resonance (NMR) ($CDCl_3$): 7.39 (t, 1-H), 7.22 to 6.96 (m, 4-H), 6.90 to 6.81 (m, 2.5-H), 6.66 (d, 0.5-H), 4.68 to 4.54 (m, 1-H), 4.21 to 4.15 (m, 1-H), 3.75 to 3.55 (m, 2-H), 2.95 to 2.71 (m, 2-H), 2.43 (br, 0.5-H), 2.21 (br, 0.5-H), 1.60 (d, 1.5-H + H_2O), 1.47 (d, 1.5-H); liquid chromatography-mass spectrometry (LC-MS): 386.0 (M^+); R_f = 0.23 (50% ethyl acetate [EtOAc]-hexanes); melting point (mp): slow >134°C. (ii) *N*-[2-(4-Fluorophenyl)-1-(hydroxymethyl)ethyl]-2(*S*)-(2,4-dichlorophenoxy)propanamide (MBX 3358) 0.142 g (87%), off-white solid; ^{1}H NMR ($CDCl_3$): 7.39 (t, 1-H), 7.22 to 6.96 (m, 4-H), 6.90 to 6.81 (m, 2.5-H), 6.66 (d, 0.5-H), 4.68 to 4.54 (m, 1-H), 4.21 to 4.15 (m, 1-H), 3.75 to 3.55 (m, 2-H), 2.95 to 2.71 (m, 2-H), 2.42 (br, 0.5-H), 2.22 (br, 0.5-H), 1.60 (d, 1.5-H + H_2O), 1.47 (d, 1.5-H); LC-MS: 386.1 (M^+); R_f = 0.23 (50% EtOAc-hexanes); mp: slow >132°C.

(ii) Synthesis of MBX 3459. 4-(Bromomethyl)-2-fluorobenzonitrile (0.100 g, 0.467 mmol, 1.0 eq) was combined with 5-methoxy-3,4-dihydro-2H-pyrrole (54 μl, 1.2 eq) in DMF (2 ml) and maintained at 50°C. After approximately 18 h, the reaction mixture was partitioned between water and DCM and separated.

The aqueous layer was extracted with additional dichloromethane (DCM; 3 times), and the combined organic layers were combined, dried ($MgSO_4$), filtered, concentrated, and purified on silica gel (0 to 100% EtOAc-hexanes) to provide 0.055 g (54%) of a light brown oil, 2-fluoro-4-[(2-oxopyrrolidin-1-yl)methyl-]benzonitrile: ^{1}H NMR ($CDCl_3$): 7.60 (t, 1-H), 7.13 (t, 2-H), 4.50 (s, 2-H), 3.31 (t, 2-H), 2.47 (t, 2-H), 2.12 to 2.02 (m, 2-H).

(iii) 2-Fluoro-4-[(2-oxopyrrolidin-1-yl)methyl]benzonitrile (0.055 g, 0.252 mmol, 1.0 eq) was combined with Raney Ni (2,800 mesh, 0.5 ml) and ammonium hydroxide (0.5 ml) in ethanol (~20 ml) and maintained under 30 lb/in^2 of H_2 gas in a Parr shaker. After approximately 18 h, the hydrogen was replaced with nitrogen, and the crude reaction mixture was filtered through Celite and concentrated to provide 0.060 g (quantitative analysis) of a white foamy solid: 1-[4-(aminomethyl) 3-fluorobenzyl]pyrrolidin-2-one: ^{1}H NMR (3:1 $CDCl_3$–deuterated methanol-d4 [MeOD-d4]): 7.30 to 7.23 (m, 1-H), 7.02 to 6.92 (m, 2-H), 4.42 (s, 2-H), 3.85 (s, 2-H), 3.66 (br, 2-H), 3.31 (t, 2-H), 2.46 (t, 2-H), 2.09 to 1.99 (m, 2-H); LC-MS: 222.8 (M^+).

(*R*)-2-(3,5-Dichloropyridy-2-oxy)butanoic acid (0.057 g, 0.229 mmol, 1.0 eq) was combined with 1-[4-(aminomethyl)-3-fluorobenzyl]pyrrolidin-2-one (0.056 g, 1.1 eq), HATU (0.104 g, 1.2 eq), and DIPEA (0.05 ml, 1.3 eq) in DMF (2 ml) and maintained at room temperature. After 36 h, the reaction mixture was diluted with water and extracted with DCM (3 times), and the combined organic layers were dried ($MgSO_4$), filtered, and concentrated *in vacuo*. The resulting residue was purified on silica gel (0 to 100% EtOAc-hexanes) to provide 0.030 g (30%) of a white foamy solid. *N*-{2-fluoro-4-[(2-oxopyrrolidin-1-yl)methyl]benzyl}-(*R*)-2-(3,5-dichloropyridin-2-yloxy)butanamide (MBX 3459): ^{1}H NMR (MeOD-d4): 7.93 (dd, 2-H), 7.28 (t, 1-H), 7.03 to 6.96 (m, 2-H), 5.12 (t, 1-H), 4.45 to 4.43 (m, 4-H), 3.36 (t, 2-H), 2.46 (t, 2-H), 2.11 to 1.97 (m, 4-H), 1.10 (t, 3-H); LC-MS: 454.0 (M^+); R_f = 0.10 (50% EtOAc-hexanes); mp: slow >63°C.

Mouse subcutaneous abscess model. The mouse model of abscess formation was performed as previously described (48). Briefly, 6- to 9-week-old C57BL/6J mice (The Jackson Laboratory, Wilmington, MA) were shaved and depilated using a topical hair remover (Nair). The mice were anesthetized with an intraperitoneal injection of ketamine and xylazine and then injected in the subcutaneous space on the left flank with the dose of bacteria indicated above in 50 μl Dulbecco's phosphate-buffered saline (DPBS). When indicated, phenoxyacetamide T3SS inhibitors were resuspended in dimethyl sulfoxide (DMSO), diluted with the bacterial suspension to a final concentration of 100 μM (final DMSO concentration, 2%), and injected into the subcutaneous space with the bacteria. Some mice were given an intraperitoneal injection of InVivo anti-mouse Ly6G (clone 1A8; BioXcell), a monoclonal antibody against Ly6G that preferentially targets neutrophils, or an IgG isotype control 48 h prior to infection. The areas of abscesses and dermonecrotic lesions were measured and calculated (long dimension × short dimension) daily for up to 2 weeks. For some mice, livers and spleens were harvested, and the soft tissues containing the abscesses were excised using an 8-mm biopsy punch. All organs and tissues were homogenized with a rotor-stator homogenizer (Omni International) in DPBS plus 0.01% Triton X-100 with cOmplete EDTA-free protease inhibitor (Roche). Serial dilutions were plated on VBM agar (49) to enumerate the CFU. The remaining soft tissue homogenate was stored at −80°C for quantification of cytokine levels. All animals were housed under standard conditions in the containment ward of the Center of Comparative Medicine at Northwestern University and were provided food and water *ad libitum*. All animal experiments were reviewed and approved by the Northwestern Animal Care and Use Committee.

Histopathology. Subcutaneous abscesses were harvested by punch biopsy at the times postinfection indicated above and immediately frozen in premium frozen section compound (VWR). Samples were sectioned and stained with hematoxylin and eosin (H&E) by the Northwestern University Mouse Histology and Phenotyping Laboratory. The stained sections were imaged under ×200 magnification using bright-field microscopy (TissueGnostics) at the Northwestern University Center for Advanced Microscopy.

Quantification of cytokines. Homogenized abscess tissues were diluted to 1 mg of protein per ml, as determined by a Bradford assay (Bio-Rad). IL-1β levels were determined by loading 100 μg/ml total protein into a MaxiSorp plate (Thermo-Fisher Scientific) and performing an enzyme-linked immunosorbent assay (ELISA) according to the manufacturer's protocol (R&D Systems). The total amount of IL-1β in each abscess was determined by multiplying the concentration of IL-1β determined by ELISA by the dilution factor used to obtain a 1-mg/ml sample.

Quantification of MPO activity. Abscess tissues were homogenized in 1 ml 50 mM phosphate (pH 6), 0.5% hexadecyltrimethylammonium bromide buffer. The homogenates were centrifuged at 18,000 × *g* for 10 min at 4°C, and the resulting supernatants were used in a myeloperoxidase (MPO) assay as a proxy for neutrophil activity. A total of 10 μl of supernatant or recombinant mouse MPO (R&D Systems) was diluted 15-fold in 50 mM phosphate (pH 6), 0.05% H_2O_2, 0.168 mg/ml *o*-dianisidine hydrochloride in a 96-well plate. The optical density at 490 nm of each well was read on a SpectraMax M3 plate reader (Molecular Devices) after 10 min. MPO activity was determined relative to the activity on a standard curve of recombinant mouse MPO activity.

Quantification of type III secretion by Western blotting. Cultures of *P. aeruginosa* were grown overnight and diluted 1:100 in LB medium supplemented with 5 mM EGTA in the presence or absence of the MBX compounds. After 4 h, cells were harvested and the proteins in the supernatant were precipitated with 20% trichloroacetic acid for 30 min on ice. Th precipitated proteins were recovered by centrifugation for 10 min at 15,000 × *g*, washed once with acetone, resuspended in Laemmli's sample buffer, and separated on a 10% SDS-polyacrylamide gel. Type III secretion proteins were detected by Western blotting using a primary antibody mix containing antibodies against the type III effectors (ExoS, ExoT, and ExoU) and translocation proteins (PopB and PopD), followed by incubation with a 1:10,000

dilution of an Alexa Fluor 680-conjugated goat anti-rabbit immunoglobulin secondary antibody (Thermo Fisher Scientific). Blots were imaged with a Li-Cor Odyssey imaging system.

Statistical analysis. Statistical analyses were performed using either unpaired *t* tests or one-way analysis of variance (ANOVA) with Dunnett's or Tukey's *post hoc* tests to adjust for multiple comparisons at a significance level of 0.05.

ACKNOWLEDGMENTS

We thank Joan Mecsas for advice and thoughtful comments.

This work was funded by grants from the National Institutes of Health: K24 AI04831 (to A.R.H.), R01 AI053674 (to A.R.H.), R44 AI068185 (to D.T.M. and A.R.H.), R01 AI099269 (to D.T.M. and A.R.H.), and CARB-X4500002329 (to D.T.M.).

REFERENCES

1. Stryjewski M, Sexton DJ. 2003. *Pseudomonas aeruginosa* infections in specific types of patients and clinical settings, p 1–15. *In* Hauser A, Rello J (ed), Severe infections caused by *Pseudomonas aeruginosa*. Kluwer Academic Publishers, Boston, MA.
2. Fiorillo L, Zucker M, Sawyer D, Lin AN. 2001. The *Pseudomonas* hot-foot syndrome. N Engl J Med 345:335–338. https://doi.org/10.1056/NEJM200108023450504.
3. Silverman AR, Nieland ML. 1983. Hot tub dermatitis: a familial outbreak of *Pseudomonas* folliculitis. J Am Acad Dermatol 8:153–156. https://doi.org/10.1016/S0190-9622(83)70017-4.
4. Solomkin JS, Mazuski JE, Bradley JS, Rodvold KA, Goldstein EJ, Baron EJ, O'Neill PJ, Chow AW, Dellinger EP, Eachempati SR, Gorbach S, Hilfiker M, May AK, Nathens AB, Sawyer RG, Bartlett JG. 2010. Diagnosis and management of complicated intra-abdominal infection in adults and children: guidelines by the Surgical Infection Society and the Infectious Diseases Society of America. Clin Infect Dis 50:133–164. https://doi.org/10.1086/649554.
5. Sievert DM, Ricks P, Edwards JR, Schneider A, Patel J, Srinivasan A, Kallen A, Limbago B, Fridkin S, National Healthcare Safety Network (NHSN) Team and Participating NHSN Facilities. 2013. Antimicrobial-resistant pathogens associated with healthcare-associated infections: summary of data reported to the National Healthcare Safety Network at the Centers for Disease Control and Prevention, 2009-2010. Infect Control Hosp Epidemiol 34:1–14. https://doi.org/10.1086/668770.
6. Rice LB. 2008. Federal funding for the study of antimicrobial resistance in nosocomial pathogens: no ESKAPE. J Infect Dis 197:1079–1081. https://doi.org/10.1086/533452.
7. Hauser AR. 2009. The type III secretion system of *Pseudomonas aeruginosa*: infection by injection. Nat Rev Microbiol 7:654–665. https://doi.org/10.1038/nrmicro2199.
8. Goehring UM, Schmidt G, Pederson KJ, Aktories K, Barbieri JT. 1999. The N-terminal domain of *Pseudomonas aeruginosa* exoenzyme S is a GTPase-activating protein for Rho GTPases. J Biol Chem 274:36369–36372. https://doi.org/10.1074/jbc.274.51.36369.
9. Pederson KJ, Vallis AJ, Aktories K, Frank DW, Barbieri JT. 1999. The amino-terminal domain of *Pseudomonas aeruginosa* ExoS disrupts actin filaments via small-molecular-weight GTP-binding proteins. Mol Microbiol 32:393–401. https://doi.org/10.1046/j.1365-2958.1999.01359.x.
10. Rangel SM, Diaz MH, Knoten CA, Zhang A, Hauser AR. 2015. The role of ExoS in dissemination of *Pseudomonas aeruginosa* during pneumonia. PLoS Pathog 11:e1004945. https://doi.org/10.1371/journal.ppat.1004945.
11. Rangel SM, Logan LK, Hauser AR. 2014. The ADP-ribosyltransferase domain of the effector protein ExoS inhibits phagocytosis of Pseudomonas aeruginosa during pneumonia. mBio 5:e01080-14. https://doi.org/10.1128/mBio.01080-14.
12. Aiello D, Williams JD, Majgier-Baranowska H, Patel I, Peet NP, Huang J, Lory S, Bowlin TL, Moir DT. 2010. Discovery and characterization of inhibitors of *Pseudomonas aeruginosa* type III secretion. Antimicrob Agents Chemother 54:1988–1999. https://doi.org/10.1128/AAC.01598-09.
13. Bowlin NO, Williams JD, Knoten CA, Torhan MC, Tashjian TF, Li B, Aiello D, Mecsas J, Hauser AR, Peet NP, Bowlin TL, Moir DT. 2014. Mutations in the *Pseudomonas aeruginosa* needle protein gene pscF confer resistance to phenoxyacetamide inhibitors of the type III secretion system. Antimicrob Agents Chemother 58:2211–2220. https://doi.org/10.1128/AAC.02795-13.
14. Williams JD, Torhan MC, Neelagiri VR, Brown C, Bowlin NO, Di M, McCarthy CT, Aiello D, Peet NP, Bowlin TL, Moir DT. 2015. Synthesis and structure-activity relationships of novel phenoxyacetamide inhibitors of the *Pseudomonas aeruginosa* type III secretion system (T3SS). Bioorg Med Chem 23:1027–1043. https://doi.org/10.1016/j.bmc.2015.01.011.
15. Pletzer D, Mansour SC, Wuerth K, Rahanjam N, Hancock RE. 2017. New mouse model for chronic infections by Gram-negative bacteria enabling the study of anti-infective efficacy and host-microbe interactions. mBio 8:e00140-17. https://doi.org/10.1128/mBio.00140-17.
16. Fleiszig SM, Wiener-Kronish JP, Miyazaki H, Vallas V, Mostov KE, Kanada D, Sawa T, Yen TS, Frank DW. 1997. *Pseudomonas aeruginosa*-mediated cytotoxicity and invasion correlate with distinct genotypes at the loci encoding exoenzyme S. Infect Immun 65:579–586.
17. Frithz-Lindsten E, Du Y, Rosqvist R, Forsberg A. 1997. Intracellular targeting of exoenzyme S of *Pseudomonas aeruginosa* via type III-dependent translocation induces phagocytosis resistance, cytotoxicity and disruption of actin microfilaments. Mol Microbiol 25:1125–1139. https://doi.org/10.1046/j.1365-2958.1997.5411905.x.
18. Thanabalasuriar A, Surewaard BGJ, Willson ME, Neupane AS, Stover CK, Warrener P, Wilson G, Keller AE, Sellman BR, DiGiandomenico A, Kubes P. 2017. Bispecific antibody targets multiple *Pseudomonas aeruginosa* evasion mechanisms in the lung vasculature. J Clin Invest 127:2249–2261. https://doi.org/10.1172/JCI89652.
19. Koh AY, Priebe GP, Ray C, Van Rooijen N, Pier GB. 2009. Inescapable need for neutrophils as mediators of cellular innate immunity to acute *Pseudomonas aeruginosa* pneumonia. Infect Immun 77:5300–5310. https://doi.org/10.1128/IAI.00501-09.
20. Cho JS, Guo Y, Ramos RI, Hebroni F, Plaisier SB, Xuan C, Granick JL, Matsushima H, Takashima A, Iwakura Y, Cheung AL, Cheng G, Lee DJ, Simon SI, Miller LS. 2012. Neutrophil-derived IL-1beta is sufficient for abscess formation in immunity against *Staphylococcus aureus* in mice. PLoS Pathog 8:e1003047. https://doi.org/10.1371/journal.ppat.1003047.
21. Becker RE, Berube BJ, Sampedro GR, Dedent AC, Bubeck Wardenburg J. 2014. Tissue-specific patterning of host innate immune responses by *Staphylococcus aureus* alpha-toxin. J Innate Immun 6:619–631. https://doi.org/10.1159/000360006.
22. Berube BJ, Rangel SM, Hauser AR. 2016. *Pseudomonas aeruginosa*: breaking down barriers. Curr Genet 62:109–113. https://doi.org/10.1007/s00294-015-0522-x.
23. Barben J, Hafen G, Schmid J, Swiss Paediatric Respiratory Research Group. 2005. *Pseudomonas aeruginosa* in public swimming pools and bathroom water of patients with cystic fibrosis. J Cyst Fibros 4:227–231. https://doi.org/10.1016/j.jcf.2005.06.003.
24. Guida M, Di Onofrio V, Galle F, Gesuele R, Valeriani F, Liguori R, Romano Spica V, Liguori G. 2016. *Pseudomonas aeruginosa* in swimming pool water: evidences and perspectives for a new control strategy. Int J Environ Res Public Health 13:E919. https://doi.org/10.3390/ijerph13090919.
25. Kang CI, Kim SH, Kim HB, Park SW, Choe YJ, Oh MD, Kim EC, Choe KW. 2003. *Pseudomonas aeruginosa* bacteremia: risk factors for mortality and influence of delayed receipt of effective antimicrobial therapy on clinical outcome. Clin Infect Dis 37:745–751. https://doi.org/10.1086/377200.
26. Koh AY, Priebe GP, Pier GB. 2005. Virulence of *Pseudomonas aeruginosa* in a murine model of gastrointestinal colonization and dissemination in neutropenia. Infect Immun 73:2262–2272. https://doi.org/10.1128/IAI.73.4.2262-2272.2005.
27. Ziegler EJ, Douglas H. 1979. *Pseudomonas aeruginosa* vasculitis and bacteremia following conjunctivitis: a simple model of fatal pseudomo-

nas infection in neutropenia. J Infect Dis 139:288–296. https://doi.org/10.1093/infdis/139.3.288.
28. Vaiman M, Lazarovitch T, Heller L, Lotan G. 2015. Ecthyma gangrenosum and ecthyma-like lesions: review article. Eur J Clin Microbiol Infect Dis 34:633–639. https://doi.org/10.1007/s10096-014-2277-6.
29. Biscaye S, Demonchy D, Afanetti M, Dupont A, Haas H, Tran A. 2017. Ecthyma gangrenosum, a skin manifestation of *Pseudomonas aeruginosa* sepsis in a previously healthy child: a case report. Medicine 96:e5507. https://doi.org/10.1097/MD.0000000000005507.
30. Goolamali SI, Fogo A, Killian L, Shaikh H, Brathwaite N, Ford-Adams M, Macfarlane S. 2009. Ecthyma gangrenosum: an important feature of pseudomonal sepsis in a previously well child. Clin Exp Dermatol 34: e180–e182. https://doi.org/10.1111/j.1365-2230.2008.03020.x.
31. Singh TN, Devi KM, Devi KS. 2005. Ecthyma gangrenosum: a rare cutaneous manifestation caused by *Pseudomonas aeruginosa* without bacteraemia in a leukaemic patient—a case report. Indian J Med Microbiol 23:262–263.
32. Zomorrodi A, Wald ER. 2002. Ecthyma gangrenosum: considerations in a previously healthy child. Pediatr Infect Dis J 21:1161–1164. https://doi.org/10.1097/00006454-200212000-00016.
33. Duncan MC, Linington RG, Auerbuch V. 2012. Chemical inhibitors of the type three secretion system: disarming bacterial pathogens. Antimicrob Agents Chemother 56:5433–5441. https://doi.org/10.1128/AAC.00975-12.
34. Quenee LE, Berube BJ, Segal J, Elli D, Ciletti NA, Anderson D, Schneewind O. 2010. Amino acid residues 196-225 of LcrV represent a plague protective epitope. Vaccine 28:1870–1876. https://doi.org/10.1016/j.vaccine.2009.11.076.
35. Quenee LE, Ciletti N, Berube B, Krausz T, Elli D, Hermanas T, Schneewind O. 2011. Plague in guinea pigs and its prevention by subunit vaccines. Am J Pathol 178:1689–1700. https://doi.org/10.1016/j.ajpath.2010.12.028.
36. Quenee LE, Ciletti NA, Elli D, Hermanas TM, Schneewind O. 2011. Prevention of pneumonic plague in mice, rats, guinea pigs and non-human primates with clinical grade rV10, rV10-2 or F1-V vaccines. Vaccine 29:6572–6583. https://doi.org/10.1016/j.vaccine.2011.06.119.
37. Faure K, Fujimoto J, Shimabukuro DW, Ajayi T, Shime N, Moriyama K, Spack EG, Wiener-Kronish JP, Sawa T. 2003. Effects of monoclonal anti-PcrV antibody on *Pseudomonas aeruginosa*-induced acute lung injury in a rat model. J Immune Based Ther Vaccines 1:2. https://doi.org/10.1186/1476-8518-1-2.
38. Moriyama K, Wiener-Kronish JP, Sawa T. 2009. Protective effects of affinity-purified antibody and truncated vaccines against *Pseudomonas aeruginosa* V-antigen in neutropenic mice. Microbiol Immunol 53: 587–594. https://doi.org/10.1111/j.1348-0421.2009.00165.x.
39. Warrener P, Varkey R, Bonnell JC, DiGiandomenico A, Camara M, Cook K, Peng L, Zha J, Chowdury P, Sellman B, Stover CK. 2014. A novel anti-PcrV antibody providing enhanced protection against *Pseudomonas aeruginosa* in multiple animal infection models. Antimicrob Agents Chemother 58:4384–4391. https://doi.org/10.1128/AAC.02643-14.
40. Francois B, Luyt CE, Dugard A, Wolff M, Diehl JL, Jaber S, Forel JM, Garot D, Kipnis E, Mebazaa A, Misset B, Andremont A, Ploy MC, Jacobs A, Yarranton G, Pearce T, Fagon JY, Chastre J. 2012. Safety and pharmacokinetics of an anti-PcrV PEGylated monoclonal antibody fragment in mechanically ventilated patients colonized with *Pseudomonas aeruginosa*: a randomized, double-blind, placebo-controlled trial. Crit Care Med 40:2320–2326. https://doi.org/10.1097/CCM.0b013e31825334f6.
41. Milla CE, Chmiel JF, Accurso FJ, VanDevanter DR, Konstan MW, Yarranton G, Geller DE, KB001 Study Group. 2014. Anti-PcrV antibody in cystic fibrosis: a novel approach targeting *Pseudomonas aeruginosa* airway infection. Pediatr Pulmonol 49:650–658. https://doi.org/10.1002/ppul.22890.
42. DiGiandomenico A, Keller AE, Gao C, Rainey GJ, Warrener P, Camara MM, Bonnell J, Fleming R, Bezabeh B, Dimasi N, Sellman BR, Hilliard J, Guenther CM, Datta V, Zhao W, Gao C, Yu XQ, Suzich JA, Stover CK. 2014. A multifunctional bispecific antibody protects against *Pseudomonas aeruginosa*. Sci Transl Med 6:262ra155. https://doi.org/10.1126/scitranslmed.3009655.
43. Hudson DL, Layton AN, Field TR, Bowen AJ, Wolf-Watz H, Elofsson M, Stevens MP, Galyov EE. 2007. Inhibition of type III secretion in *Salmonella enterica* serovar Typhimurium by small-molecule inhibitors. Antimicrob Agents Chemother 51:2631–2635. https://doi.org/10.1128/AAC.01492-06.
44. Slepenkin A, Chu H, Elofsson M, Keyser P, Peterson EM. 2011. Protection of mice from a *Chlamydia trachomatis* vaginal infection using a salicylidene acylhydrazide, a potential microbicide. J Infect Dis 204: 1313–1320. https://doi.org/10.1093/infdis/jir552.
45. Shaver CM, Hauser AR. 2004. Relative contributions of *Pseudomonas aeruginosa* ExoU, ExoS, and ExoT to virulence in the lung. Infect Immun 72:6969–6977. https://doi.org/10.1128/IAI.72.12.6969-6977.2004.
46. Hoang TT, Kutchma AJ, Becher A, Schweizer HP. 2000. Integration-proficient plasmids for *Pseudomonas aeruginosa*: site-specific integration and use for engineering of reporter and expression strains. Plasmid 43:59–72. https://doi.org/10.1006/plas.1999.1441.
47. Wolfgang MC, Lee VT, Gilmore ME, Lory S. 2003. Coordinate regulation of bacterial virulence genes by a novel adenylate cyclase-dependent signaling pathway. Dev Cell 4:253–263. https://doi.org/10.1016/S1534-5807(03)00019-4.
48. Inoshima N, Wang Y, Wardenburg JB. 2012. Genetic requirement for ADAM10 in severe *Staphylococcus aureus* skin infection. J Investig Dermatol 132:1513–1516. https://doi.org/10.1038/jid.2011.462.
49. Vogel HJ, Bonner DM. 1956. Acetylornithinase of *Escherichia coli*: partial purification and some properties. J Biol Chem 218:97–106.